Desalination and Water Treatment
www.deswater.com

doi:10.5004/dwt.2016.0059

59 (2017) 144–153
January

Removal of Cr(VI) and Zn(II) from an aqueous solution using an organic-inorganic composite of bentonite-biochar-hematite

Elvis Fosso-Kankeu*, Frans. B. Waanders, Frederik W. Steyn

School of Chemical and Minerals Engineering of the North West University, Potchefstroom; South Africa, Tel. +2718 299 1659, Fax +2718 299 1535, email: kaelpfr@yayoo.fr (E. Fosso-Kankeu), frans.Waanders@nwu.ac.za (F.B. Waanders), steynfw@gmail.com (F.W. Steyn)

Received 15 January 2016; Accepted 10 June 2016

ABSTRACT

A bentonite/biochar/hematite composite was synthesized to develop an adsorbent with the properties of each constituent suitable for the removal of Cr(VI) and Zn(II) from aqueous solution. The composite was prepared through slow pyrolysis and characterized using scanning electron microscope (SEM) and X-ray fluorometry (XRF). The developed adsorbent was used in a batch system for the removal of individual metal ion of Cr(VI) and Zn(II). The XRF results showed that the composite contained the elements found in the respective constituents, while the SEM results showed that the morphology of the composite resulted from the combination of the constituents, indicating a successful synthesis of the composite. The adsorption study showed the affinity of bentonite and biochar for the Zn(II) which was mainly due to the negative groups present in those adsorbents, while hematite with a net positive charge was mainly suitable for the removal of Cr(VI) present as dichromate in the working pH range (between 6 and 8). The adsorption behaviour of the adsorbent fitted the Freundlich isotherm model implying that the adsorption mostly occurred through a heterogeneous binding of metal to the surface of the adsorbent. The composite did not exhibit the highest adsorption capacity but was the only adsorbent capable to remove both Cr(VI) and Zn(II), with an adsorption capacity of 5.414 mg/g and 5.167 mg/g respectively. The composite could therefore be used for the treatment of wastewater contaminated by both metals.

Keywords: bentonite/biochar/hematite composite; Adsorption; Metal ion; Kinetic; Isotherm; Scanning electron microscope

1. Introduction

The main metal pollutants that are released from some industries into the water systems include Pb(II), Cu(II), Cd(II), Ni(II), Cr(VI) and Zn(II) [1]. With specific levels of pH and temperature, these metals are soluble in water, contaminating the water sources [2]. These metals pose a great threat to the environment and the organisms depending on the water source.

Hexavalent chromium compounds are 10–1000 times more toxic than trivalent chromium. Chromate and dichromate anions form at pH level between six and eight; they are soluble in water and could be easily distributed along the river network [3]. The hexavalent chromium (Cr(VI)) has been reported as one of the commonly hazards which is carcinogenic and mutagenic to human [4–8]. A strict guideline limiting the level of Cr(VI) in groundwater to 50 μg L^{-1} has been established by the World Health Organization [9], as the exposure to contaminated water may lead to DNA damage [10], mutations [11], chromosomal aberrations [12] and carcinomas of the respiratory organs [13].

Zinc is not a carcinogenic compound and has poor mobility, thus infection only occurs close to the source of contamination. This compound is known to cause irritation and corrosion of the gastrointestinal tract and acute renal tubular necrosis. The high toxicity and non-degradable nature of these metals contribute to the impact they have on the environment and should be removed completely or the concentration should be reduced to sufficient levels [14].

Several techniques have been applied for the removal of metal contaminants from polluted water, however, adsorp-

*Corresponding author.

tion has emerged as one of the most attractive techniques due to its low cost, simplicity and Eco friendliness. The adsorbent composition is arguably the most important factor determining the efficiency of an adsorption process. The effectiveness of the other factors is influenced by the physico-chemical composition of the adsorbent [15]. Bentonite is a natural clay that can be found in many countries around the world and is particularly of interest in adsorption studies for its abundance, economic viability and heavy metal adsorption properties [16]. Bentonite clay can be formed in situ by the alteration of volcanic ash. It consists of two silicate tetrahedral sheets between an aluminium octahedral sheet. The clay has a permanent negative charge which is often balanced by cations, such as sodium and calcium, occurring in the lattice structure [17]. Bentonite clay has been found to effectively adsorb many different pollutants including heavy metals and even greenhouse gasses [18]. The permanent negative charge of the clay is what gives it its great adsorption capacity and potential, but is also the largest potential drawback if negatively charged ions have to be adsorbed [19].

Hematite is commonly classified as a nanoscale metal oxide (NMO) material, which is a group of metallic compounds known for their high surface area and adsorption capacity [20]. NMOs rarely exist in pure form and contain many impurities, such as aluminium, silicon and manganese, which will affect the outcome of experiments. For this reason, hematite is normally precipitated from an iron solution with a base to ensure purity and subsequently, accuracy in all experiments. NMOs are rarely used in their pure form and are usually supported by another adsorbent to limit the agglomeration of the molecules in an aqueous solution [15,21]. Hematite is well known for the strong adsorption affinity toward Cr(VI) [22]. When supported by other adsorbents, the high adsorption capacity intrinsic to hematite can be realised. NMOs tend to agglomerate in aqueous solutions due to the strong Van der Waal's forces between the large surface area of the NMO and the water molecules. This in turn limits the adsorption potential and therefore limits its uses in aqueous solution [22].

Biochar is a carbon-rich material that is produced by pyrolysis of biomass [20]. The versatility and availability of biochars or derived composites are unmatched by other adsorbents [23]. Biochars that are used for adsorption are normally pyrolysed under temperatures lower than 550°C to prevent the destruction of the phenolic bonds that aid in the adsorption process [24]. Due to the functional groups and low cost of formation, biochars have shown high cost effectiveness for the adsorption of heavy metals [23]. The nature of biochar formation however makes it difficult to produce the same adsorbent in repeating experiments [23], but this disadvantage is far outweighed by the cost effectiveness of this adsorbent.

Composites of organic clays and biochar have been prepared in previous studies in an attempt to increase the amount of pollutants that can be adsorbed compared to the pure adsorbents [22,25]. NMO and bentonite composites have shown reasonably good results in previous studies. The two components complement each other in that they address the short-comings of each other to produce an overall improved adsorbent [21]. Biochar and NMO composites have been actively studied, especially the magnetic variants. The adsorption effectiveness is increased to a large extent, despite some draw backs that can be associated with these composites [26,27]. As shown by Wang et al. [26], the adsorption effectiveness of a biochar/hematite composite for lead increased by a factor of 20 compared to the pure substances. The electrostatic interactions caused by the hematite are amplified by the number of active sites that are available when the NMO is supported [26]. A composite containing clay, biochar (made from rosin) and NMO was prepared by Ruan et al. [22] and has shown phenomenal results for the adsorption of Cr(VI). This composite has shown to have an adsorption efficiency nearly ten times larger for Cr(VI) than any of the constituent compounds or their composites [22]. A previous study [28] has shown that the nature of the biomass significantly affects the physicochemical composition of the biochar derived from it. It is therefore obvious that a replicate of the above composite with a different biomass will exhibit different properties and affinity toward metals.

The aim of the present study is to prepare such a composite from the sweet sorghum bagasse then characterize the composite using XRF and SEM for surface morphology. The adsorption behaviour and capacity of the prepared composite for the removal of Cr(VI) and Zn(II) from an aqueous solution in a batch adsorption experiment system was then determined using kinetic and isotherm models.

2. Methodology

2.1. Materials

The natural bentonite clay used in this study was obtained from Yellowstar bentonite mine, near Koppies in the Free State South Africa. The clay was ground and sieved to achieve a particle size smaller than 150 µm.

The batch of sweet sorghum bagasse was obtained from the College of Agriculture in Potchefstroom-South Africa. It was ground and sieved to achieve a particle size smaller than 150 µm.

Ferric-chloride hexahydrate ($FeCl_3 \cdot 6H_2O$) was purchased from associated chemical enterprises (ACE). The compound was dissolved in deionised water and different processes were applied for the various composites to form the hematite particles.

The two salts used to prepare the metallic solutions in this study included potassium dichromate ($K_2Cr_2O_7$) and Zinc chloride ($ZnCl_2$) which were purchased from ACE as analytical grade reagents.

2.2. Preparation of adsorbents

2.2.1. Bentonite/biomass (Bt/Bm)

The bentonite and biomass were combined in a 1:5 mass ratio, and then pyrolysed at 400°C (in the presence of nitrogen) to form a powdered sample. This sample was crushed and sieved once again to obtain a particle size smaller than 150 µm.

2.2.2. Bentonite/hematite (Bt/Hem)

Eleven grams of bentonite were added to 26 mL of deionised water. The ferric-chloride hexahydrate was added in a 1:1 mass ratio to the aqueous bentonite solution. A 5 M sodium hydroxide solution was added drop wise to facilitate the precipitation of the hematite, and subsequently

passed through a filter to remove the excess water from the adsorbent. The solid retentate was dried at 70°C overnight in the oven. The product was crushed and sieved to obtain a particle size smaller than 150 µm.

2.2.3. Biomass/hematite (Bm/Hem)

The biomass and ferric-chloride hexahydrate were combined in a 1:1 mass ratio in 64 mL of deionised water. A 5 M sodium hydroxide solution was added drop wise to facilitate the precipitation of the hematite, and subsequently passed through a filter to remove the excess water from the adsorbent. It was then pyrolysed at 400°C (in the presence of nitrogen) to form a powdered sample that was then crushed to a particle size smaller than 150 µm.

2.2.4. Bentonite/Biomass/hematite (Bt/Bm/Hem)

The bentonite/biomass/hematite were combined in a 1:4:1.5 mass ratio to form a mixture and a 5 M ammonium hydroxide solution was added drop wise to facilitate the precipitation of the hematite [22]. This solution was passed through a filter and continuously washed. The retentate was then pyrolysed at 400°C (in a nitrogen atmosphere). The product was crushed and sieved to obtain a particle size smaller than 150 µm.

2.2.5. Control groups

The pure bentonite control was dried, crushed and sieved to obtain a particle size smaller than 150 µm, whilst the biomass was pyrolysed and treated to obtain similar particle size. The hematite control was formed by precipitation of the iron oxide in the presence of ammonium hydroxide.

2.2.6. Summary

In Table 1 the amount of each material required to form the various adsorbents is shown.

2.3. Preparation of adsorptive solutions

2.3.1. Synthetic metallic solutions

The synthetic metallic solutions were prepared by dissolving the salts of potassium chromate and zinc chloride in separate containers with distilled water to form a stock solution of 1000 mg L^{-1}. This stock solution was subsequently diluted with distilled water of a given volume to form the corresponding working solution used in the adsorption experiment.

Table 1
Summary of components needed for the formation of the composites

Material	Bt (g)	Bc (g)	Hem (g)	Bt/Bc (g)	Bt/Hem (g)	Bc/Hem (g)	Bt/Bc/Hem (g)
Bt	12.8	–	–	5.12	10.67	–	3.46
Bm	–	43.67	–	25.6	–	25.6	25.6
$FeCl_6H_20$	–	–	64	–	10.67	25.6	15.36
Water	–	–	160	–	26.67	64	38.4

2.4. Adsorption experiments

All adsorption experiments were carried out in a batch system using the 250 mL Erlenmeyer flasks. The flask containing the metallic solution and the adsorbent was incubated in a temperature controlled incubator shaker set at 200 rpm for a given time keeping the pH unchanged.

2.4.1. Adsorption with different initial metal concentrations

An amount of 0.1 g of adsorbent was added to 25 mL of adsorptive solutions and continuously stirred at 200 rpm for 1 h. The adsorbate concentrations in solution were 25, 50, 75 and 100 mg L^{-1}. The suspension was centrifuged at 4000 rpm for 10 min.

The supernatant was removed with a pipette and the residual concentration of the metal ion was determined using the inductively coupled plasma optical emission spectrometer (ICP Expert II, Agilent Technologies 720 ICP-OES).

2.4.2. Adsorption of metals at various contact times

The results from the isotherm study were used to determine the composite with the highest adsorption capacity for hexavalent chromium and zinc; the best composite was further used in the adsorption kinetics experiments to confirm its potential.

The adsorbent (0.1 g) was added to a 25 mL solution containing 50 mg L^{-1} of metal ion. This solution was stirred at 200 rpm for 15, 30, 45 and 60 min, and samples were extracted at each time interval. The extracted samples were centrifuged at 4000 rpm for 10 min and the supernatants were removed by a pipette and the residual concentrations of the metal ions were determined using the inductively coupled plasma optical emission spectrometer (ICP Expert II, Agilent Technologies 720 ICP-OES).

2.5. Mathematical modelling

The modelling of the adsorption behaviour was done in two phases namely Isotherm modelling and kinetic modelling.

Before applying these models, the equilibrium concentration of the adsorbate must first be found experimentally and the adsorption capacity determined using Eq. (1);

$$q_i = \frac{(C_0 - C_i)V}{m} \tag{1}$$

where q_i is the amount of metal adsorbed per unit mass of adsorbent (mg/g); C_0 is the initial concentration of the metal ions in the solution (mg L^{-1}); C_i is the metal ion concentration (mg L^{-1}) ; m is the amount of adsorbent (g) and V is the solution volume (L). The subscript "i" denotes the state of the system, either equilibrium (e) or at a time interval (t).

2.5.1. Isotherm modelling

The Langmuir isotherm as described by [29–31];

$$q_e = \frac{KQC_e}{1+KC_e} \tag{2}$$

Or in linearized form;

$$\frac{C_e}{q_e} = \frac{1}{KQ} + \frac{C_e}{Q} \tag{3}$$

where q_e is the amount of metal adsorbed per unit mass of adsorbent (mg/g); C_e is the metal ion concentration at equilibrium (mg L^{-1}) ; K is the adsorption coefficient and Q is the maximum capacity (mg/g).

The Freundlich isotherm is described by Yao et al. [25]:

$$q_e = k_f C_e^{1/n} \tag{4}$$

Or in linearized form;

$$\ln q_e = \ln k_f + \frac{1}{n}\ln C_e \tag{5}$$

where q_e is the amount of metal adsorbed per unit mass of adsorbent (mg/g); C_e is the metal ion concentration at equilibrium (mg L^{-1}); k_f is the adsorption coefficient and n is a constant for the model.

2.5.2. Kinetic modelling

Before applying the kinetic models, the adsorption capacity at different times need to be calculated according to the equation described above.

The pseudo first order kinetic rate law is described by Yao et al. [25] as:

$$\frac{dq_t}{dt} = k_1\left(q_e - q_t\right) \tag{6}$$

The pseudo second-order kinetic rate law is given by:

$$\frac{dq_t}{dt} = k_2\left(q_e - q_t\right)^2 \tag{7}$$

where k_1 and k_2 are the rate constants for the first and second order kinetics, respectively. Non-linear regression methods will be used to determine these rate constants.

2.6. Characterization of the adsorbents

2.6.1. X-ray fluorometry (XRF)

The elemental composition of the clay was determined using the X-ray fluorometer (XRF), the analysis was performed on the MagiX PRO & SuperQ Version 4 (Panalytical, Netherland); a rhodium (Rh) anode was used in the X-ray tube and operated at 50 kV and current 125 mA; at power level of 4 kW.

2.6.2. Scanning electron microscopy (SEM)

The morphology of the adsorbent composites was determined by scanning electron microscope (SEM) photographs from a TECSAN, model VEGA 3 XMU from the Czech Republic, with a 10 micron lens.

3. Results and discussion

3.1. Elemental composition of the adsorbents

The XRF analysis of the seven adsorbents showed that the chemical composition varied among the pure clay and the synthesized adsorbents. Table 2 indicates the most prominent compounds that are present in the adsorbents.

The high mass percentage of iron oxide in the hematite containing adsorbents indicates that insertion of hematite on the newly synthesized adsorbent was successful. The presence of silicone oxide is attributed to both the biochar and the bentonite clay. The XRF analysis does not account for carbon-based compounds.

3.2. Morphology of the adsorbents

The SEM image of the biochar at one thousand-time magnification is displayed as Fig. 1(a). The biochar mainly consists of rod-like structures that have many alcoves and protrusions. According to the study performed by Yin et al. [32], the formation of these porous cylindrical structures may be attributed to the formation and subsequent expulsion of volatile components.

The SEM image of the bentonite/biochar composite at one thousand-times magnification is displayed as Fig. 1(b). Similarly, to that of the biochar control group, rod-like structures and protrusions are the most dominants. However, unlike the control group, bentonite particles can be seen in the image as small lumps. The surface texture is not as smooth as that of the control group and would have a larger surface area.

A one thousand-times enlarged image of the bentonite/hematite composite is shown in Fig. 1(c). The hematite appears to have formed crystalline structures that are attached to the surface of the clay and can be seen throughout the entire image due to its characteristic plate-like hexagonal crystalline structure. The morphology presented in this study is near identical to the morphology observed by Al-Farhan [33].

Fig. 1(d) shows the biochar/hematite composite at a magnification of one thousand times. Small crystalline structures are slightly visible, which indicates that hematite formed successfully on the surface. The hematite is not as easily observed compared to the bentonite/hematite composite. The size of the hematite particles in this composite is significantly smaller than that of the bentonite/hematite composite.

Table 2
Mass percentage of compounds in the adsorbents

Component	Bc	Bt	BtBc	BcHem	BtHem	BtBcHem
Al_2O_3	0.79	18.68	1.63	4.18	3.32	16.78
SiO_2	38.38	62.89	52.51	38.84	23.13	55.54
K_2O	29.94	2.58	17.25	17.82	2.39	2.32
CaO	12.59	1.82	9.27	7.05	0.83	0.42
Fe_2O_3	4.29	10.86	5.97	20.53	67.02	17.67

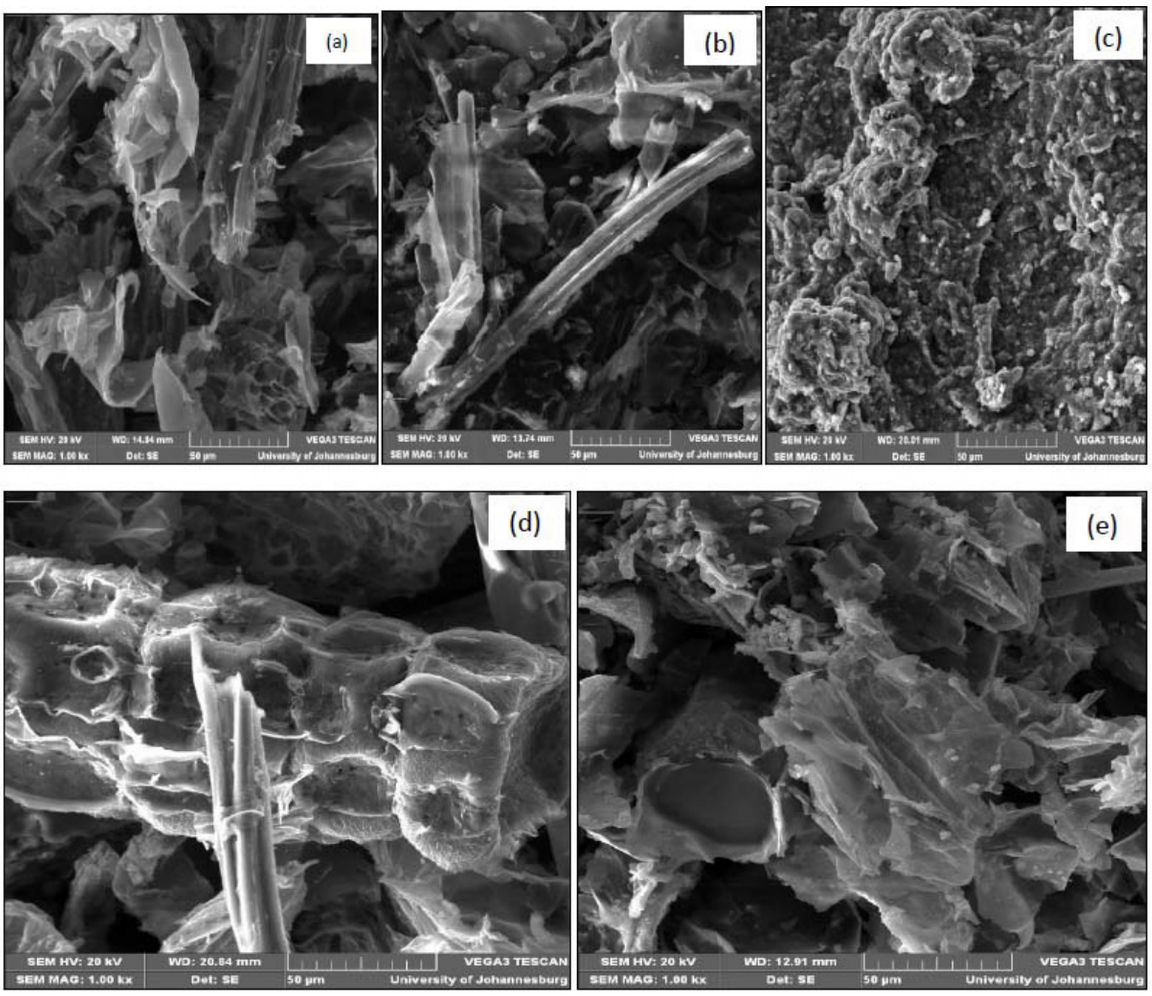

Fig. 1. SEM micrograph of: (a) biochar, (b) bentonite/biochar, (c) bentonite/hematite, (d) biochar/hematite and (e) bentonite/biochar/hematite.

A one thousand-times magnification of the bentonite/biochar/hematite composite revealed that the formation process was successful. The image is displayed as Fig. 1(e). The bentonite granules adhered to the biochar more successfully compared to the bentonite/biochar composite. A larger amount of hematite particles are attached to the biochar in this composite as compared to the biochar/hematite composite. As proposed by Ruan et al. [22], the hematite may serve as binding agent between the biochar and bentonite. Small bentonite granules are seen in a very large area of the image, proper formation and adhesion of hematite to the surface also occur.

3.3. Adsorption study

Following the method described previously, seven adsorbents and their accompanying adsorptive solutions were prepared. Isotherm adsorption studies were performed in accordance to the description in methodology. The data was analysed to determine the best composite to be used for the kinetic study.

3.3.1. Isotherm study

The models frequently used for the isotherm study include the Freundlich isotherm model which describes a heterogeneous layer adsorption and the Langmuir isotherm model which describes a monolayer adsorption. The isotherms parameters are obtained by plotting $\log(q_e)$ versus $\log(C_e)$ for the Freundlich model, and C_e/q_e versus C_e for the Langmuir model.

The adsorption study results were fitted to the linearized Freundlich and Langmuir isotherm models and the results are displayed in Table 3.

3.4. Adsorption behaviour of simple adsorbents

3.4.1. Bentonite

Adsorption equilibrium data for the removal of Cr(VI) from solution were fitted to the Freundlich isotherm model and the coefficient of determination obtained was close to unity ($R^2 = 0.938$); while the fitness of these data to the Langmuir isotherm model resulted to a lower coefficient of determination ($R^2 = 0.6795$). The Freundlich isotherm model was

Table 3
Summary of isotherm parameters

Adsorbent	Adsorption of Cr(VI)				Adsorption of Zn(II)			
	Best model	Parameters		q_e (mg/g)	Best model	Parameters		q_e (mg/g)
Bt	Freundlich	kf	0.023	0.291	Freundlich	kf	1.184	14.536
		n	1.529			n	1.56	
		R^2	0.938			R^2	0.9525	
Bc	Freundlich	kf	0.005	0.529	Freundlich	kf	2.384	14.063
		n	0.855			n	2.204	
		R^2	0.936			R^2	0.9775	
Hem	Langmuir	Q	21.321	17.24	Langmuir	Q	0.389	0.312
		kf	0.085			kf	0.082	
		R^2	0.925			R^2	0.92	
Bt/Bc	Freundlich	kf	0.003	0.572	Freundlich	kf	3.251	10.897
		n	0.733			n	3.234	
		R^2	0.853			R^2	0.851	
Bt/Hem	Freundlich	kf	0.184	1.518	Langmuir	Q	2.697	1.953
		n	1.852			kf	0.053	
		R^2	0.978			R^2	0.91	
Bc/Hem	Freundlich	kf	0.006	0.979	Freundlich	kf	0.173	5.087
		n	0.755			n	1.156	
		R^2	0.93			R^2	0.928	
Bt/Bc/Hem	Langmuir	Q	9.648	7.075	Freundlich	kf	0.01	4.917
		kf	0.055			n	0.626	
		R^2	0.982			R^2	0.924	

therefore suitable to describe the adsorption of Cr(VI) and was subsequently used to determine the isotherm parameters. Using computerized linear regression methods the calculated adsorption coefficient and exponent were 0.023 and 1.529, respectively. The adsorption potential was calculated and a value of 0.291 mg/g was obtained.

For the adsorption of Zn(II), the Langmuir and Freundlich isotherm models were found to fit (R^2 = 0.9515 and 0.9525, respectively) the adsorption equilibrium data. Since the values of the coefficients of determination are nearly identical and closer to unity, the adsorption of Zn(II) on the bentonite occurred both onto homogeneous and heterogeneous surfaces. The calculated adsorption coefficient and exponent were 1.184 and 1.56, respectively. The adsorption potential was calculated as 14.536 mg/g.

The maximum adsorption capacity of bentonite for the removal of Zn(II) from solution is nearly 50 times larger than when removing Cr(VI) from solution. This discrepancy can be attributed to the cationic nature of Zn(II) and a hydroxyl functional group that is found in this particular bentonite [1]. The anionic structure of the dichromate ion ($Cr_2O_7^{2-}$) creates a repulsion force between it and the hydroxyl group, limiting surface contact and thus effectively reducing its adsorption. According to a study by Sag et al., [34], the statistical mechanics and kinetic gas theory are important factors when interpreting adsorption behaviour data. The probability of surface contact, and thus adsorption, increases as the compound's atomic weight increases because of the kinetic energy it possesses. In this study however, the kinetic and the probability theory will not be accounted for because the kinetic energy difference between the species is vastly offset by the ionic charge difference.

3.4.2. biochar

The biochar was used to adsorb Cr(VI) and the equilibrium data was fitted to the Freundlich and Langmuir isotherm models, and the coefficient of determination values obtained as 0.936 and 0.337, respectively. The adsorption of Cr(VI) by the biochar could be therefore predicted using the Freundlich model. The results obtained in Table 3 indicate that the values of the adsorption coefficient and exponent are 5.44 x 10^{-3} and 0.855, respectively. The calculated adsorption potential was 0.529 mg/g.

The adsorption of Zn(II) by the biochar is best described by the Freundlich model which has a determination coefficient of 0.9775. The adsorption coefficient and exponent values calculated were 2.3835 and 2.204, respectively. The adsorption potential derived from the intercept was 14.063 mg/g.

Biochar outperformed bentonite for the removal of Zn(II) and could therefore be considered as a valid alternative in regions were pure bentonite is not available or expensive. The adsorption potential for Zn(II) is 25 times larger than the value calculated for Cr(VI) adsorption. The functional groups in the biochar are mainly responsible for this enormous difference. According to a study performed by Lawrinenko [35], carbonyl and carboxylate functional

groups are commonly produced by fast pyrolysis resulting in a negatively charged surface. This would in part, explain the high adsorption affinity of biochar for Zn(II) and the low adsorption affinity towards Cr(VI).

3.4.3. Hematite

Hematite was formed according to the procedure described in the methodology and was used for the removal of Cr(VI); the Langmuir and Freundlich models were fitted to the adsorption equilibrium data. The isotherm parameters are summarized in Table 3. The Langmuir isotherm model for the adsorption of Cr(VI) had the highest coefficient of determination of 0.925, compared to the Freundlich model and was therefore suitable for the prediction of the adsorption behaviour. The adsorption constant was calculated as 0.0845 with a maximum adsorption potential value of 21.321 mg/g. The value of the adsorption potential derived from the intercept was 17.24 mg/g.

The adsorption of Zn(II) by hematite was well expressed by the Langmuir isotherm model with a better fit to the experimental data (R^2 = 0.92). An adsorption coefficient of 0.0815 was obtained and the maximum adsorption capacity was 0.389 mg/g. The adsorption potential of the hematite in this case was 0.312 mg/g.

It has been shown throughout the literature that hematite has a uniquely high adsorption affinity for Cr(VI) [36]. The highly cationic nature of the hematite mineral is the principal factor contributing to the observed adsorption affinity toward Cr(VI), specifically the dichromate ion. The same argument could be considered to explain the lower adsorption affinity toward the positively charged Zn(II) ion.

3.5. Adsorption behaviour of composites

3.5.1. Bentonite/biochar composite

The Cr(VI) removal behaviour has been explained earlier and it is not surprising that the bentonite/biochar composite has an equally low adsorption capacity for Cr(VI). The isotherm data is shown in Table 3. The Freundlich isotherm model showed a coefficient of determination of 0.853, which is higher than that of the Langmuir model. The calculated adsorption coefficient and exponent were 0.003 and 0.733, respectively. The calculated value of the adsorption potential was 0.572 mg/g.

The isotherm study of the adsorption of Zn(II) showed that both the Langmuir and the Freundlich isotherm models had a relatively low coefficient of determination (R^2 = 0.851). The Freundlich isotherm model had a smaller deviation between runs and was chosen as the model that best describes the system. The corresponding parameters could be determined based on the Freundlich isotherm model. The values obtained for the adsorption coefficient and the exponent were 3.251 and 3.234, respectively. The adsorption potential was calculated and gave a value of 10.897 mg/g. This value is 33% smaller than that of the biochar and bentonite as simple adsorbents.

It is possible that the anionic functional groups of the biochar partially bind with the cationic functional groups of the bentonite and vice versa. Another possible reason for the discrepancy between the composite's adsorption capacity and that of its constituents is due to the obstruction of pores caused by the addition of bentonite. This reduces the amount of available adsorption sites and lowers the adsorption potential of the composite.

3.5.2. Bentonite/hematite composite

The averaged isotherm data from the adsorption of Cr(VI) by the bentonite/hematite composite are shown in Table 3. The Langmuir model best describes the adsorption behaviour, with a coefficient of determination of 0.978. The calculated adsorption coefficient and exponent were 0.1835 and 1.8515, respectively. The value obtained for the adsorption potential was 1.518 mg/g.

The adsorption of Zn(II) is best described by the Langmuir isotherm model with a corresponding coefficient of determination of 0.91. The maximum adsorption capacity and the adsorption constant obtained were 2.697 and 0.0525, respectively. The adsorption potential of the bentonite/hematite composite was 1.953 mg/g.

The composite performed poorly compared to its separate constituents, due to the inhibition of functional groups available in the structure of the individual compounds. The cationic nature of the hematite and the anionic nature of the bentonite are naturally attracted to one another. The binding between the functional groups of the two compounds severely limit the available surface area needed for successful adsorption. This phenomenon confirms why the SEM images showed such a large number of hematite crystals on the bentonite surface. The advantage of excellent adhesion between the two minerals is offset by the disadvantage of a vastly reduced adsorption potential for either metal.

3.5.3. Biochar/hematite composite

Results in Table 3 show that the adsorption of Cr(VI) is better expressed by the Freundlich isotherm model (R^2 = 0.930). The values of the calculated adsorption coefficient and exponent were 5.5 x 10^{-3} and 0.755, respectively. The corresponding adsorption potential was found to be 0.979 mg/g.

The Freundlich isotherm model was found to be the best model to describe the adsorption of Zn(II) yielding a coefficient of determination value of 0.928. Computed values of the adsorption coefficient and exponent were 0.1725 and 1.156, respectively. The adsorption potential was calculated, and a value of 5.087 mg/g was obtained.

The low adsorption potential of the composite toward Cr(VI) is due to the similar phenomenon observed with the bentonite/biochar composite. The functional groups of the biochar bind with those of the hematite and effectively saturate the surface. The SEM images showed that only a small amount of hematite was attached, reinforcing the statement that the hematite might be saturated. This causes the hematite to be nearly irrelevant in the adsorption process, even more so than in the bentonite/hematite composite. The adsorption potential of the composite toward Zn(II) is relatively high. Comparing it to the bentonite/hematite composite it is seen that the biochar/hematite composite outperforms it. Bentonite and biochar both have similar adsorption potentials for each ion, but greatly different potentials when combined with hematite. The discrepancy could be attributed to the biochar's organic nature that has far less cationic functional groups

due to the high percentage of organic molecules typically found in plant material.

3.5.4. Bentonite/biochar/hematite composite

The isotherm study of the adsorption of Cr(VI) showed that the adsorption behaviour was best described by the Langmuir isotherm model and the corresponding coefficient of determination of 0.982 was obtained.

The maximum adsorption capacity was 9.648 mg/g and the adsorption constant was 0.055. The adsorption potential of this composite was calculated from the slope of the linear equation and yielded a value of 7.075 mg/g. This is the highest value for the adsorption of Cr(VI) by any composite.

Studying the adsorption of Zn(II) it can be seen (Table 3) that the Freundlich isotherm model has the highest coefficient of determination value of 0.924. The adsorption coefficient and exponent were calculated as 0.01 and 0.626, respectively. The calculated value of the adsorption potential was 5.167 mg/g.

3.5.5. Kinetics study

It is important to determine the rate and the mechanisms of an adsorption process such as to be able to optimize the process for large scale implementation. Two kinetic models namely the pseudo-first and -second order kinetic models are often used to determine the kinetic parameters relevant for the interpretation of the rate limiting step of the adsorption process.

3.5.6. Biochar

A kinetic study of the adsorption behaviour of Zn(II) by biochar was conducted. The biochar displayed a high adsorption affinity toward Zn(II), second only to bentonite. The biochar was however chosen because it is considered as the main basis of the composite.

The study was performed as described in the methodology. Pseudo first- and -second order kinetic models were used to describe the adsorption behaviour. Fig. 2 (run 1 and run 2) shows the results for both runs and each kinetic model.

The averaged model parameters calculated from the data as displayed in Fig. 2 are shown in Table 4.

In both cases, a very high coefficient of determination was found. The overall coefficient of determination for the pseudo first order model was 0.986, which was lower than for the pseudo second order model (R^2 = 0.994). The adsorption coefficient (k_2) for the second order model was found to be 0.015 and the adsorption potential was 9.1 mg/g. Although this model has the largest coefficient of determination, the difference between the calculated and experimental adsorption capacity was 13.15%, while a difference of only 0.83% was observed in the case of the pseudo first order model.

3.5.7. Bentonite/biochar/hematite composite

A kinetic study was performed for the removal of Cr(VI) from solution by the composite. Pseudo-first and -second order models were used to describe this system. Table 5 shows the averaged data from this study.

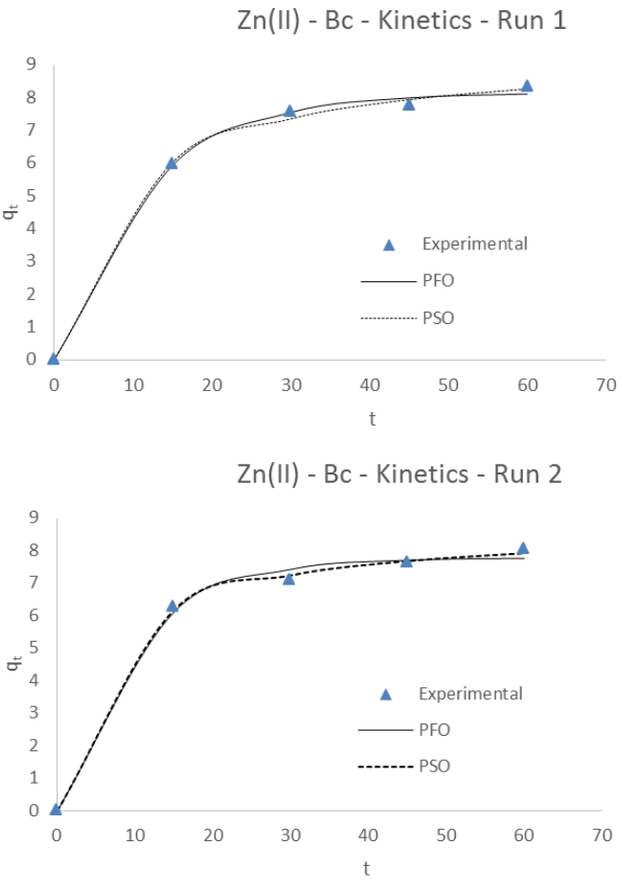

Fig. 2. Pseudo first- and second order plot for Zn(II) adsorption on biochar (Run 1 and Run 2).

Table 4
Calculated parameters of the kinetic models for Zn(II) adsorption onto biochar

Kinetic model	Model parameters	Values
Pseudo-first order	k_1 (min^{-1})	0.094
	q_{e1} (mg/g)	7.975
	R^2	0.986
Pseudo-second order	k_2 (g mg^{-1}.mol^{-1})	0.015
	q_{e2} (mg/g)	9.100
	R^2	0.994

Fig. 3 shows the results for both runs and fitting of each kinetic model.

In both cases, a very high coefficient of determination was found. The overall R^2 value for the pseudo-first order model was determined as 0.979, whereas a R^2 value of 0.975 was determined for the pseudo second order. The adsorption coefficient for the pseudo-first order model was found to be 0.0434 and the adsorption potential was 5.414 mg/g. The calculated adsorption potential differs from the experimental value by only 6.4%.

The bentonite/biochar/hematite composite's adsorption capacity is approximately two and half times less than the best performing adsorbent for either adsorptive solution.

It is the second best adsorbent for Cr(VI) and the best composite adsorbent for the same metal. This could be because of the larger amount of hematite that adhered to the composite, as illustrated by the SEM images. Because of this, the hematite active sites might not be fully saturated as was the case with the other hematite-containing adsorbents.

The composite is the third least effective adsorbent for Zn(II), and performing far less than the second least effective. The greater amount of hematite in the adsorbent limits the adsorption potential of the composite because the functional groups have the same charge as the Zn(II) ion. However, the amount of hematite present in the composite is not enough to totally inhibit the adsorption of Zn(II). The high affinity of the bentonite and biochar to Zn(II) is mainly responsible for the observed adsorption potential.

This composite could be an alternative to the use of many adsorbents to clean a specific system. Although it does not absorb Cr(VI) like hematite or Zn(II) like biochar or bentonite, it is the only adsorbent in this study to effectively adsorb both metallic ions.

Table 5
Calculated parameters of the isotherm models for Cr(VI) adsorption on bentonite/biochar/hematite

Kinetic model	Model parameters	Values
Pseudo-first order	k_1 (min^{-1})	0.043
	q_{e1} (mg/g)	5.414
	R^2	0.979
Pseudo-second order	k_2 (g mg^{-1}.mol^{-1})	0.005
	q_{e2} (mg/g)	7.339
	R^2	0.975

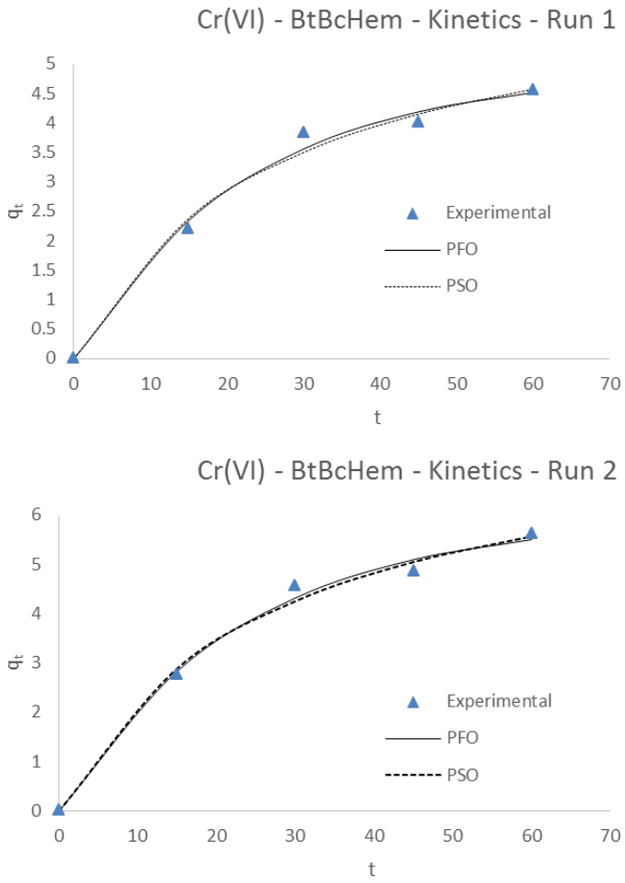

Fig. 3. Pseudo first- and second order plot for Cr(VI) adsorption on bentonite/biochar/hematite.

4. Conclusion

The formation and characterization of the composites were successful and the SEM images provided visual evidence. The isotherm study exhibited mixed results, but overall, the Freundlich isotherm described the systems in the best manner, implying that the mechanism of metals adsorption was dominated by binding to heterogeneous surface for most of the adsorbents [37]. The biochar is well suited for Zn(II) adsorption, rivalling even bentonite. It can be considered as a valid alternative in regions where pure bentonite is hard to obtain. The adsorption potential for Zn(II) is 25 times larger than the value calculated for Cr(VI) adsorption. The negative charge of functional groups in the biochar are mainly responsible for this enormous difference. Bentonite and biochar appear to function in a similar manner regarding adsorption. The composite, however, had a lower adsorption capacity for Zn(II) than either of its constituents. Although the bentonite/biochar/hematite did not exhibit the highest adsorption capacity for either of the metal ion, it was the only adsorbent capable to remove both Cr(VI) and Zn(II) and could therefore be recommended for polishing in hybridized treatment system of wastewater contaminated by both metals.

Acknowledgement

The authors are grateful to the sponsor from the North-West University and the National Research Foundation (NRF) in South Africa. Any opinion, findings and conclusions or recommendations expressed in this material are those of the authors and therefore the NRF does not accept any liability in regard thereto. The contribution of Mr N. Lemmer is really appreciated.

References

[1] E. Fosso-Kankeu, C.M. Van der Berg, F.B. Waanders, Physico-chemical activation of South African bentonite clay and impact on metal adsorption capacity, 6th International Conference on Green Technology, Renewable Energy and Environmental Engineering (ICGTREEE'2014), 27–28 November 2014, Cape Town-South Africa, E. Muzenda, S. Sandhu, eds., (2014) pp 247–252.

[2] K.G. Bhattacharyya, S.S. Gupta, Adsorptive accumulation of Cd(II), Co(II), Cu(II), Pb(II), and Ni(II) from water on montmorillonite: influence of acid activation, J. Colloid Interface Sci., 310(2) (2007) 411–424.

[3] Q. Cheng, C. Wang, K. Doudrick, C.K. Chan, (2015) Hexavalent chromium removal using metal oxide photocatalysts, Appl. Catal. B: Environ., 1(177) (2015) 740–748.
[4] L. Hu, Y. Cai, G. Jiang, Occurrence and speciation of polymeric chromium (III), monomeric chromium (III) and chromium (VI) in environmental samples, Chemosphere, 156 (2016) 14–20.
[5] T. Santonen, A. Zitting, V. Riihimaki, P.D. Howe, M. Wood, Concise International Chemical Assessment Document 76: Inorganic Chromium (III) Compounds (2009).
[6] D. Metze, N. Jakubowski, D. Klockow, Speciation of chromium. In: R. Comelis, H. Crews, J. Caruso, K.G. Heumann (Eds.), Handbook of Elemental Speciation II: Speciation in the Environment, Food, Medicine & Occupational Health. John Wiley & Sons, Ltd (2005).
[7] M.A. Stewart, P.M. Jardine, M.O. Barnett, T.L. Mehlhorn, L.K. Hyder, L.D. McKay, Influence of soil geochemical and physical properties on the sorption and bioaccessibility of chromium (III), J. Environ. Qual., 32 (2003) 129– 137.
[8] IARC, IARC Monographs on the Evaluation of Carcinogenic Risks to Humans, vol. 49. Chromium, Nickel and Welding (1990).
[9] WHO, Chromium in drinking-water. Background Document for Preparation of WHO Guidelines for Drinking-water Quality, World Health Organization, Geneva, (WHO/SDE/WSH/03.04/4) (2003).
[10] E. Peterson-Roth, M. Reynolds, G. Quievryn, A. Zhitkovich, Mismatch repair proteins are activators of toxic responses to chromium-DNA damage, Mol. Cell. Biol., 25 (2005) 3596–3607.
[11] A. Leonard, R.R. Lauwerys, Carcinogecity and mutagenicity of chromium, Mutat. Res. Rev. Genet., 76 (1980) 227–239.
[12] F. Majone, and A.G. Levis, Chromosomal aberrations and sister-chromatid exchanges in chinese hamster cells treated in vitro with hexavalent chromium compounds, Mutat. Res. Rev. Genet. Toxicol., 67 (1979) 231–238.
[13] T. Fang, X. Yang, L. Zhang, J. Gong, Ultrasensitive photoelectrochemical determination of chromium (VI) in water samples by ion-imprinted/formate anion-incorporated graphitic carbon nitride nanostructured hybrid, J. Hazard. Mater., 312 (2016) 106–113.
[14] R. Donat, A. Akdogan, E. Erdem, H. Cetisli, Thermodynamics of Pb^{2+} and Ni^{2+} adsorption onto natural bentonite from aqueous solutions, J. Colloid Interface Sci., 286(1) (2005) 43–52.
[15] Z. Orolínová, and A. Mockoviaková (2009) Structural study of bentonite/iron oxide composites, Mater. Chem. Phys., 114(2–3) (2009) 956–961.
[16] Y. Chen, Adsorption of La(III) onto GMZ bentonite: effect of contact time, bentonite content, pH value and ionic strength, J. Radioanal. Nucl. Chem., 3(292) (2012) 1339–1347.
[17] T.S. Anirudhan, and M. Ramachandran, Adsorptive removal of basic dyes from aqueoussolutions by surfactant modified bentonite clay(organoclay): Kinetic and competitive adsorption isotherm, Process Saf. Environ. Prot., 1(95) (2015) 215–225.
[18] D.J.L. Guerra, I. Mello, L.R. Freitas, R. Resende, R.A.R. Silva, Equilibrium, thermodynamic, and kinetic of Cr(VI) adsorption using a modified and unmodified bentonite clay, Int. J. Mining Sci. Tech., 1 (24) (2014) 525–535.
[19] C. Yong-Gui, H. Yong, Y. Wei-Min, J. Ling-Yan, Competitive adsorption characteristics of Na(I)/Cr(III) and Cu(II)/Cr(III) on GMZ bentonite in their binary solution, J. Ind. Eng. Chem., 1(26) (2014) 335–339.
[20] X. Shuibo, Z. Chun, Z. Xinghou, Y. Jing, X. Zhang, W. Jingsong, Removal of uranium (VI) from aqueous solution by adsorption of hematite, J. Environ. Radioact., 1 (100) (2009) 162–166.
[21] A. Dimirkou, A. Loannou, N. Doula, Preparation, characterization and sorption properties for phosphates of hematite, bentonite and bentonite–hematite systems, Adv. Colloid Interface Sci., 1 (97) (2002) 37–61.
[22] Z.-H. Ruan, J.-H. Wu, J.-F. Huang, Z.-T. Lin, Y.-F. Li, Y.-L. Liu, P.-Y. Cao, Y.-P. Fang, J. Xie, G.-B. Jiang, Facile preparation of rosin-based biochar coated bentonite for supporting α-Fe_2O_3 nanoparticles and its application for Cr(VI) adsorption, J. Mater. Chem. A., 3 (8) (2015) 4595–4603.
[23] X. Tan, Y. Liu, G. Zeng, X. Wang, X. Hu, Y. Gu, Z. Yang, Application of biochar for the removal of pollutants from aqueous solutions, Chemosphere, 125 (2015) 70–85.
[24] A. Liu, Y. Park, Z. Huang, B. Wang, R.O. Ankunah, P.K. Biswas Product identification and distribution from hydrothermal conversion of walnut shells, Energ. Fuels, 20 (2006) 446–454.
[25] Y. Yao, B. Gao, J. Fang, M. Zhang, H. Chen, Y. Zhou, A.E. Creamer, Y. Sun, L. Yang, Characterization and environmental applications of clay–biochar composites, Chem. Eng. J., 242 (2014) 136–143.
[26] S. Wang, B. Gao, Y. Li, A. Mosa, A.R. Zimmerman, L.Q. Ma, W.G. Harris, K.W. Migliaccio, Manganese oxide-modified biochars: Preparation, characterization, and sorption of arsenate and lead, Bioresour. Technol., 181 (2015) 13–17.
[27] S. Wang, B. Gao, A.R. Zimmerman, Y. Li, L. Ma, W.G. Harris, K.W. Migliaccio, Removal of arsenic by magnetic biochar prepared from pinewood and natural hematite, Bioresour., Technol., 175 (2014) 391–395.
[28] Y. Lee, J. Park, C. Ryu, K.S. Gang, W. Yang, Y.-K. Park, J. Jung, S. Hyun, Comparison of biochar properties from biomass residues produced by slow pyrolysis at 500°C, Bioresour. Technol., 148 (2013) 196–201.
[29] E. Fosso-Kankeu, A.F. Mulaba-Bafubiandi, B.B. Mamba, T.G. Barnard, Prediction of metal-adsorption behaviour in the remediation of water contamination using indigenous microorganisms, J. Environ. Manage., 92(10) (2011) 2786–2793.
[30] H. Mittal, E. Fosso-Kankeu, S.B. Mishra, A.K. Mishra, Biosorption potential of Gum ghatti-g-poly (acrylic acid) and susceptibility to biodegradation by *B. subtilis*, Int. J. Biol. Macromol., 62 (2013) 370–378.
[31] E. Fosso-Kankeu, H. Mittal, S.B. Mishra, A.K. Mishra, Gum ghatti and acrylic acid based biodegradable hydrogels for the effective adsorption of cationic dyes, J. Ind. Eng. Chem., 22 (2015) 171–178.
[32] R. Yin, R. Liu, Y. Mei, W. Fei, X. Sun, Characterization of bio-oil and bio-char obtained from sweet sorghum bagasse fast pyrolysis with fractional condensers, Fuel, 112 (2013) 96–104.
[33] B.S. Al-Farhan, Potential removal of crystal violet (CV), acid red (AR) and methyl orange (MO) from aqueous solution by magnetic nanoparticles, Int. J. Nanomater. Chem., 1(3) (2015) 97–102.
[34] Y. Sag, B. Akeael, T. Kutsal, Ternary biosorption equilibria of Cr(VI), Cu(II) and Cd(II) on Rhizopus arrhizus, Sep. Sci. Technol., 37 (2002) 279–309.
[35] M. Lawrinenko, Anion exchange capacity of biochar. Thesis in Master of Science at the Iowa State University, Department of Agronomy, (2014).
[36] H.I. Adegoke, F. AmooAdekola, O.S. Fatoki, B.J. Ximba, Adsorption of Cr(VI) on synthetic hematite (α-Fe_2O_3) nanoparticles of different morphologies, Sep. Technol. Thermody., 31(1) (2013) 142–154.
[37] A.O. Dada, J.O. Ojediran, A.P. Olalekan, Sorption of Pb^{2+} from aqueous solution unto modified rice husk: Isotherms studies, Adv. Phys. Chem., (2013) 1–6.